IOP Conference Series: Materials Science and Engineering

PAPER • **OPEN ACCESS**

Development of plasma actuators for re-ignition of aeroengine under high altitude conditions

To cite this article: Ghazanfar Mehdi *et al* 2022 *IOP Conf. Ser.: Mater. Sci. Eng.* **1226** 012034

Development of plasma actuators for re-ignition of aeroengine under high altitude conditions

Ghazanfar Mehdi[1], Bonuso Sara[1], De Giorgi Maria Grazia [1]*

[1] University of Salento, Department of Engineering for Innovation, Lecce, Italy

*mariagrazia.degiorgi@unisalento.it

Abstract. Re-ignition of aeroengine under high altitude conditions is of great importance to the safety and use of lean-burn engines. The present work investigated the experimental and numerical analysis of flow and re-ignition characteristics in a rectangular burner. A ring-needle type plasma actuator was developed and powered by high voltage nanopulsed plasma generator with different percentage values of amplitude voltage and frequencies. Flow visualizations by using high speed camera and Proper Orthogonal Decomposition (POD) were performed to recognize the dominant flow structures. Experimental results showed the transport effects such as induced flow with an impact on the recirculation zone near the corners of combustor, improving the mixing performance, which could be contribute to the reduction of ignition delay timings. Experimental characterization in non-reactive flow allowed the estimation of the electrical power and the optimal reduced electric field (E_N) value, which was then used as input to the numerical study for the flame ignition analysis. Ignition characteristics were analyzed by coupling two different numerical tools ZDPlasKin and Chemkin. It was noticed that time required to achieve the maximum flame temperature with plasma actuation is significantly reduced in compared with autoignition timings (clean case). Maximum reduction in ignition timings was observed at inlet pressure 1 bar (3.5×10^{-5} s) in respect to clean case (1.1×10^{-3} s). However, as the inlet pressure is reduced, the ignition delay timings were increased. At 0.6 bar flame ignition was occurred at 0.0048s and 0.0022s and in clean case and plasma actuation case, respectively.

1. Introduction

Air safety regulations are increasing day by day which insisted the gas turbine manufacturers to address the re-ignition problems at high altitude conditions. Recently, Non-thermal plasma (NTP) is considered as a most prominent technique to improve the ignition and combustion by shortening the ignition delay timings, increasing lean flame stabilization, improving engine performance, accelerating low-temperature oxidation, extending lean blowout limits and reducing emissions [1, 2]. Non-thermal plasma has great capability to augment the ignition and combustion process by thermal (via temperature rise), kinetic (via plasma generated electronically and vibrationally excited molecules and active radicals) and transport ways: diffusion transport enhancement effect via fuel decomposition and low temperature oxidation and convective transport enhancement due to plasma generated ionic wind, hydrodynamic instability, and flow motion via Coulomb and Lorentz forces [3].

Successful demonstrations of plasma assisted ignition has been performed by using different NTPs such as micro wave discharge, atmospheric pressure discharge, radio frequency discharge, corona discharge, direct current glow discharge (DCGD), surface discharge, laser ignition and dielectric

barrier discharge (DBD) [4]. However, DBD plasma actuators showed great interest in aeronautics due to reattaching of separated flows and controlling of boundary layer from transition to turbulence [5, 6]. Moreover, it is cheap to build, light weight, reduce the noise of aircraft, easy to handle and function at real time operating conditions. The arrangement of DBD is based on two electrodes; one is connected with high voltage while the other is grounded [4]. Basically, DBD is working into two different operations modes i-e sinusoidal wave form and nanosecond repetitively pulsed discharge (NRPD). Mainly, NRPD has been shown great interest due to effective and wide capacity of generating excited states and active radicals by ionization, dissociation, and electron impact excitation reactions by means of high E_N which enhanced the flame ignition [7]. Moreover, NRPD also generate the fast gas heating which helps to improve the ignition via improvement in thermal pathways [8]. However, during the NRPD electron impact reactions (plasma chemistry) have different time scales than the gas phase reactions (combustion chemistry) [9].

Bernard [10, 11] conducted the experimental investigations to examine the effects of DBD on turbulent air jet driven by sinusoidal generator. The turbulent spectrum, turbulent kinetic energy, and velocity profiles have been analyzed, it was also noticed that DBD plasma actuation could lead to improve the mixing performance. Xu [12] studied the impacts of AC-DBD in coaxial burner with an inner tube carrying air jet and an outer tube containing CH_4 jet. During the tests, an outer burner tube is surrounded with high voltage electrode whereas an inner burner tube is acted as a grounded electrode. Before the mixing of methane and air, AC-DBD was subjected to the fuel (methane). The authors noticed that flame structure was enormously reliant on the edge reduced electric field generated by means of AC-DBD.

Besides it, many experimental and numerical researches were performed to develop kinetic model including plasma actuated reactions and observed ignition enhancement by NRPD. Kosarev [13] studied the numerical and experimental techniques to analyze the ignition kinetics of CH_4: O_2: Ar mixture at temperature ranges of 1230 K to 1719 K and pressure of 0.3 bar to 1.1 bar by subjecting high voltage NRDP in the Shock tube. It has been proved that ignition timing was considerably reduced with the use of NRDP. However, this study neglected the evolution of vibrational and electronical excitation species. Starik [14] investigated the combustion mechanism of methane–air mixture including kinetics of singlet oxygen but ignores the modeling of plasma discharge and vibrational species. Uddi [15] performed the experimental and comparative measurements of oxygen atom in air and methane–air mixture subjecting NRDP by using laser induced fluorescence, but they neglected the treatment of vibrational species.

Although, many studies have been performed during the last decade, but the accurate mechanism and fundamental knowledge of ignition enhancement is still at exploratory stages, it could be possible with the optimization of each specific process involved in the plasma assisted ignition. The present work investigated the experimental and numerical study of flow dynamics and re-ignition characteristics in a rectangular burner, particularly under the low pressure conditions. However, the re-ignition of aeroengine under high altitude conditions is of great importance to the safety and use of lean-burn. A ring-needle type plasma actuator was considered and run by high voltage nanosecond pulsed generator by varying the magnitudes of applied voltage in order to distinguish the effects of each specific process on flow dynamics. The comparative analysis of electrical characterization in the absence of flame was performed. Smoke flow visualization was carried by using high resolution camera to analyse the fluid dynamics effects of plasma actuation on the flow behaviour. POD analysis was also performed to recognize the major flow structures produced at different plasma actuation conditions. Finally, ignition characteristics were analysed by coupling two different numerical tools ZDPlasKin and Chemkin.

2. Experimental setup and electrical characterization

The experimental setup was implemented to analyse the impacts of NRPD on the flow behaviour and electrical characteristics as shown in Figure 1. A ring-needle plasma actuator was installed in the rectangular burner and driven by nanosecond pulsed generator. The plasma actuator composed of two

copper electrodes. The ring type electrode with the inner diameter = 32 mm and outer diameter = 52mm, was connected to the high voltage. The ground electrode is given by a needle type electrode with length of 330 mm and diameter equal to 1 mm, placed at the center of ring type electrode at standoff distance s = 0 mm. The standoff distance referred to the position of needle electrode from the upper edge of ring electrode. The experimental tests were performed considering non-reactive flow at atmospheric temperature and pressure. A faraday cage was used to protect the instrumentation from electromagnetic field. Table 1 shows the plasma actuator test conditions, in terms of percentage value of voltage amplitude and frequency. The electrical setup comprised of high voltage nanosecond pulsed generator, current transformer, HV probe, oscilloscope and a personal computer. The current transformer and HV probe were connected to oscilloscope to analyse the time depended curves of voltage and current.

Table 1. Experimental conditions.

Test Case	Actuator configuration		Actuation conditions			Standoff Distance (mm)
No.	**High voltage**	**Ground**	**Generator**	**Amplitude (% V_{max})**	**Frequency (% F_{max})**	
1.	Disk	Needle	Nanopulsed Generator	20%	30%	00
2.				40%	30%	00

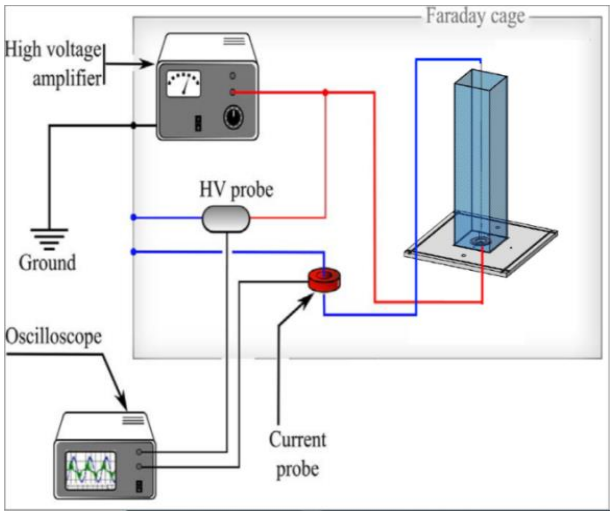

Figure 1. A detailed sketch of experimental setup and electrical characterization.

3. Numerical procedure

Chemical kinetic modeling of plasma assisted ignition has been performed by coupling a zero-dimensional plasma kinetic model (ZDPlasKin) [16] and the chemical kinetic model (CHEMKIN) [17]. ZDPlasKin solver was considered to predict the thermal and kinetic effects of NRPS on the air and methane-air mixture. The Boltzmann equation solver was integrated with ZDPlaskin to analyze the evolution of time dependent species. The results obtained from ZDPlaskin were integrated with CHEMKIN. Finally, CHEMKIN was used to examine the ignition delay timings particularly at high altitude conditions i-e low-temperature and pressure. The closed homogenous batch reactor was used for ignition analysis. The extended version of plasma chemical kinetic mechanism of methane-air was compiled from the literature by considering both electron impact reactions and gas phase reactions [18-21]. The detailed mechanism included charged transfer reactions, vibrationally excited reactions, electronically excited reactions, three body recombination reactions, ionization, relaxation, and

dissociation reactions. The detailed description of numerical procedure and experimental validation of extended version of mechanism has been presented in our previously published articles [2, 22, 23].

4. Results and discussions

4.1 Electrical characterization

Table 2 presented the plasma actuation conditions and mean electrical power delivered to the non-reactive flow. It has been observed that thermal power delivered to fluid is almost same in Test case 1 and 2. The temporal evolution of the voltage-current characteristics and E_N of Test case 1 are shown in Fig. 2. The voltage signal is highly variable due to the NRPD actuation. The current signals present several high-amplitude spikes. These spikes are due to discharges that lead to a fast electrical impedance change within the actuator. The E_N value was estimated by considering the acquired voltage signal and the gap distance between the ring and needle electrodes. The mean integral value of E_N of Test 1 was calculated about 200 Td by underlining the several peaks during the single pulse discharge. The main reason behind the selection of Test 1, because it has been proved previously, ignition delay timings have been enhanced at 200 Td [2, 22, 23]. Therefore, numerical analysis of ignition characteristics has been performed by considering the electrical output of Test 1.

Table 2. Electrical output of different test cases.

Test Case No.	Voltage peak (V)	Repetition Rate (Hz)	Pulse Electrical Power (W)	Mean Electrical Power (W)	Uncertainty Pulse Electrical Power (W)
1.	14152.01	813.6697	644.4663	1.2581	70
2.	16795.8	755.287	660.782	1.1974	70

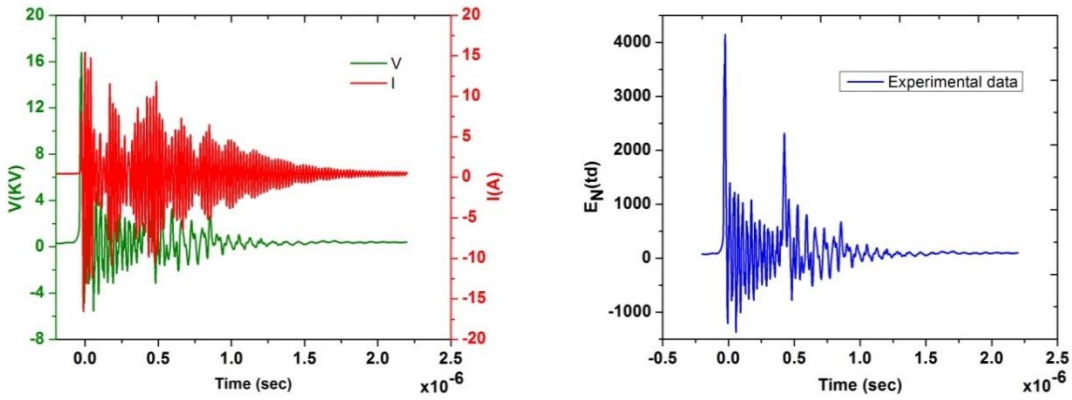

(a) **(b)**

Figure 2. Electrical characterization for the Test case 1 (a) Voltage V(t) and current I(t) curves (b) reduced electric field (E_N).

4.2 Flow visualization

Flow visualization has been carried out by using a high resolution camera (MEMRECAM GX-3). An advantage of the analysis under quiescent conditions is that it is possible to observe some features of the induced flow which otherwise would be swept away by an external flow. Comparison of smoke flow visualizations at the downstream region of the exposed electrodes at different amplitudes (Tests 1-2) were performed for the identification of vortical flow pattern generated in quiescent atmospheric air by the plasma actuator were shown in Fig 3. It has been

noticed that the in test 1 and test 2, flow field was uniformly distributed, only one leading vortex was observed on the corners of closed box that could be used to induce the recirculation of the flow in the application in burners, leading to the combustion control through this aerodynamic effect.

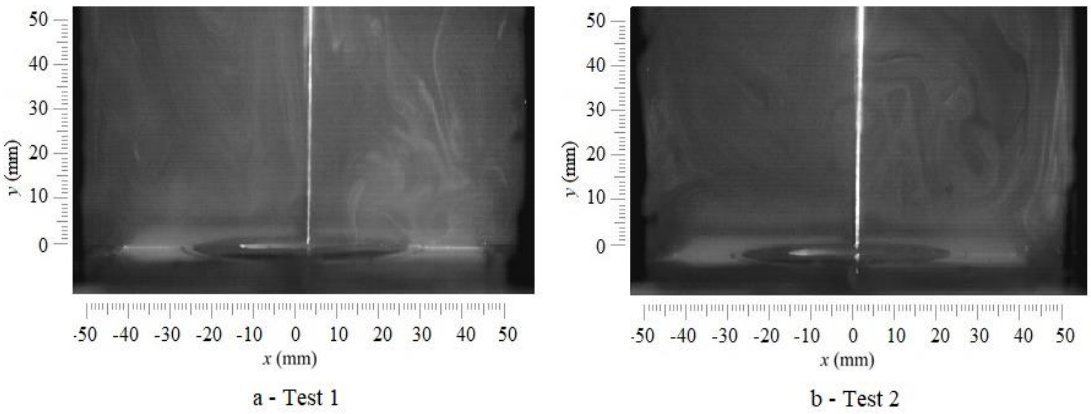

Figure 3. Comparative analysis of smoke flow visualization at different amplitudes (Test 1 and 2).

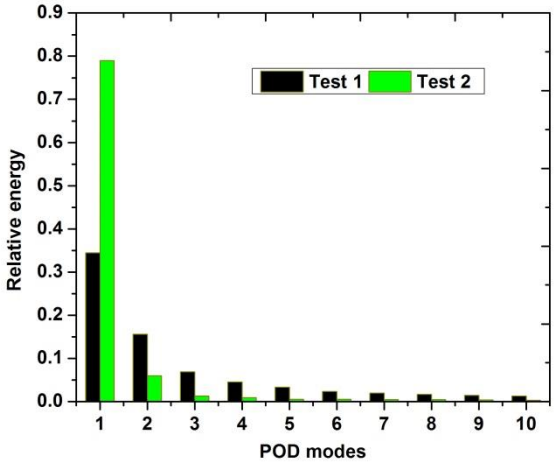

Figure 4. Comparative analysis of relative energy of first 10 modes of Test 1 and 2.

Adding to this, for the better understanding of flow vortexes and coherent structures, POD analysis of non-reactive flow were performed which allows the identification of dominant structures from random data. The sign and the intensity of POD eigen structures represented the flow coherent structures. They owned the relative energy which is proportional to the contribution of each mode to the flow field reconstruction. Prior to the analysis of POD based structures it is compulsory to measure the criteria of broadness of modes which have almost all the relative energy. It was estimated that the relative energy is mainly consumed and distributed by the first three modes in all tests cases as shown in Fig 4. Though, the influence of 1st mode was relatively high. It was concluded that POD modes above number 3 present a negligible impact on the POD structures. Hence, only first three modes were considered for the flow analysis. The POD structures at different amplitudes are shown in Fig 5. In test 1, Mode 1 and Mode 2 were more symmetric because they have less relative energy difference as in Fig 4. However, in test 2, Mode 1 and Mode 2 were quite different structure because almost 80% of relative energy was captured by Mode 1. Besides this, flow recirculation was guite attached with the

needle electrode as in Test 1 and 2 it could be due the less standoff distance (0mm) between ring and needle electrode.

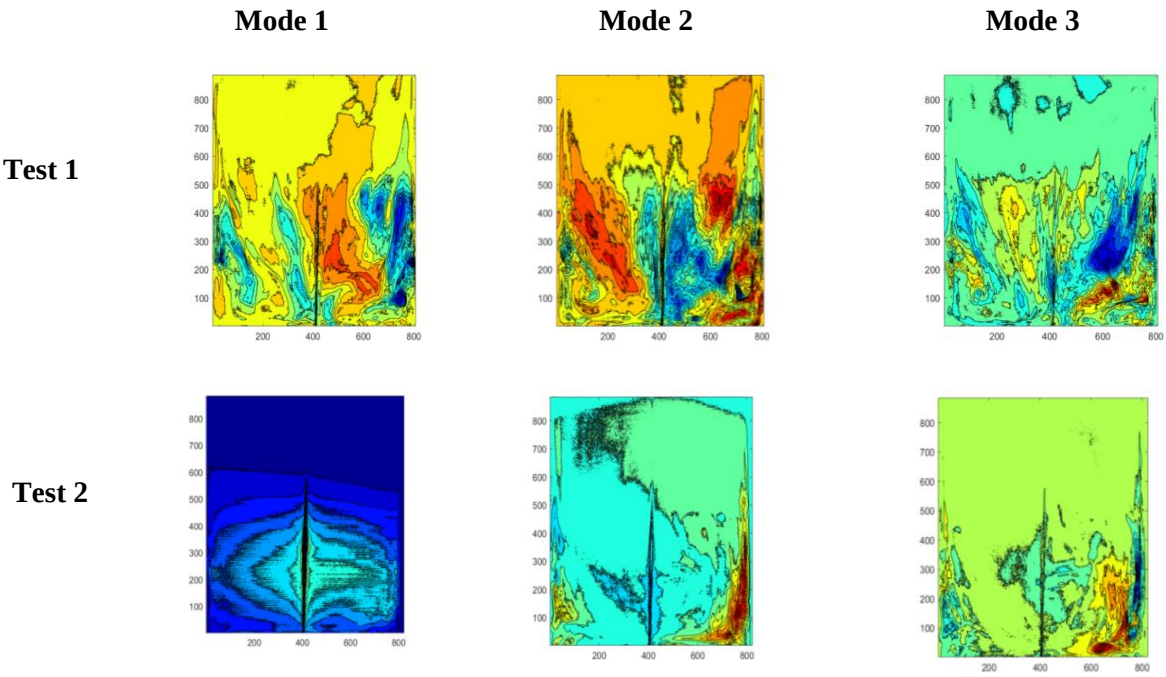

Figure 5. POD analysis of first three modes of Test 1 and 2.

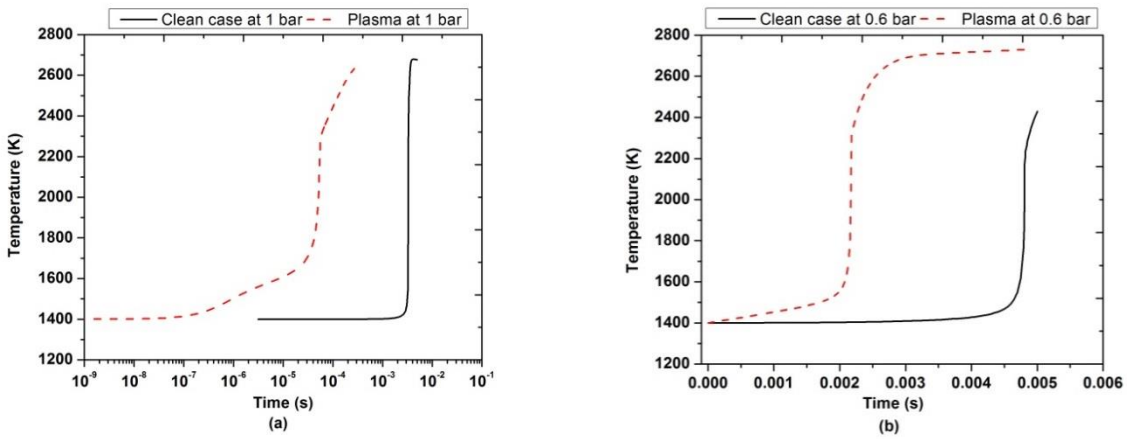

Figure 6. Comparative behaviour of ignition characteristics of clean case (black line) with plasma actuation (red dashed line) at low pressure conditions (a) 1 bar (b) 0.6 bar (c) 0.4 bar considering constant inlet temperature 1400 K, E_N 200 Td, and stoichiometric conditions.

4.3 Ignition characteristics at low pressure conditions.

The plasma actuator effects in combustor have been characterized in terms of thermal effects, kinetic effects, and transport effects. Experiments showed that the plasma needle-disk plasma actuator influenced the fluid dynamics with an induced flow and a possible impact on the recirculation zone near the corners of combustor, improving the mixing performance of mixture, which could be contribute to the reduction of ignition delay timings. ZDPlasKin was used to investigate the effects of plasma actuation at the same experimental E_N as of Test 1. Finally, the ZDPlasKin results in terms of thermal and kinetic effects were coupled with Chemkin 2021 R1. A closed homogeneous batch reactor

(CHBR) was used to estimate the ignition delay timings. Figure 6 showed the comparative analysis of ignition delay timings of clean case with plasma actuation at different inlet pressures by putting constant inlet temperature and E_N. It was noticed that the time required to achieve the maximum flame temperature with plasma actuation is significantly reduced in comparison with autoignition timings (clean case). At inlet of pressure of 1 bar a reduction in ignition timings was achieved with plasma (3.5×10^{-5} s) in comparison to clean case (1.1×10^{-3} s). However, lowering the inlet pressure, the ignition delay timings of clean and plasma actuation were increased. At 0.6 bar flame ignition occurred in clean case at (0.0048s) and plasma actuation (0.0022s). The ignition enhancement is due to the conversion of electron energy into the bond energy of free/active radicals produced during the plasma discharge processes. Then, the bond energy of free/active radicals is transformed into internal energy during the ignition process.

5. Conclusion

The present work investigated the experimental and numerical characterization of flow structures and ignition delay timings particularly at high altitude conditions i-e low inlet pressure. Plasma assisted ring-needle plasma actuator was developed and operated with nanosecond plasma generator. The comparative behavior of electrical characterization has been performed at two different percentage value of amplitude and frequency at the standoff distances of 0mm. The mean power and an optimum value of E_N were predicted, which could be essential for numerical study of ignition delay timings. Smoke flow visualization and POD results showed the transport effects of plasma actuation which influenced the fluid dynamics. The plasma induced flow could have an impact on the recirculation zone near the corners of combustor, and a possible improvement of the mixing of the mixture, which could be contribute to the reduction of ignition delay timings. Finally, an analysis was performed to compare the ignition delay timings of clean case and the cases with plasma actuation at two different inlet pressures and constant inlet temperature and E_N. It was noticed that the time required to achieve the maximum flame temperature with plasma actuation is significantly reduced in comparison to autoignition timings (clean case). Maximum reduction in ignition timings was observed at inlet pressure 1 bar, in particular the plasma actuation leads to an ignition timing of 3.5×10^{-5} s while the clean case of 1.1×10^{-3} s. However, lowering the inlet pressure, the ignition delay timings of clean and plasma actuated cases were increased. At 0.6 bar flame ignition was occurred at 0.0048s and 0.0022s in clean case and plasma actuation case, respectively.

Funding Acknowledgements

- The work was supported and funded by the PON R&I 2014 - 2020 Asse I "Investimenti in Capitale Umano" Azione I.1 "Dottorati Innovativi con caratterizzazione industriale" - Corso di Dottorato in "Ingegneria dei Sistemi Complessi" XXXV ciclo - Università degli Studi del Salento" - Borsa Codice: DOT1312193 n. 3.
- This project is also received funding from the Clean Sky 2 Joint Undertaking (JU) under the grant aggrement N. 831881 (CHAiRLIFT). The JU recieves support from the European Union's Horizon 2020 research and innovation programme and the Clean Sky 2 JU members other than the Union.

References

[1] Starikovskiy A and Aleksandrov N 2013 *Progress in Energy and Combustion Science* **39** 61-110.
[2] Mehdi G, De Giorgi M G, Fontanarosa D, Bonuso S and Ficarella A 2021 *Proceedings of the ASME Turbo Expo* **V03B**T04A036.
[3] Starikovskiy S M 2006 *J.Phys. D Appl. Phys*. **39 (16)** 265-299.
[4] Ruma M, Ahasan H and Ranipet H B 2016 *Int. J. Renew. Energy Environ. Eng*. **04 (01)** 006-012.
[5] De Giorgi M G, Pescini E, Marra F and Ficarella A 2016 *Appl. Therm. Eng*. **106** 334-350.
[6] Francioso, De Pascali C, Pescini E, De Giorgi M G and Siciliano P 2016 *J. Phys. D: Appl. Phys*. **49 (23)** 235201.
[7] Ju Y and Sun W 2015 *Progress in Energy and Combustion Science* **48** 21-83.
[8] Tholin F and Lacoste D A and Bourdon A 2014 *Combustion and Flame* **161 (5)** 1235-1246.
[9] Aleksandrov N L, Kindysheva S V, Kukaev E N, Starikovsjaya S M and Starikovskii A Y 2009 *Plasma Physics Reports* **35 (10)** 867-882.
[10] Bernard N, Braud P, Pons J, Touchard G and Moreau E 2007 *J. Turbul*. **8 (49)** 1-24.
[11] Bernard N, Bonnet J P, Touchard G and Moreau E 2008 *AIAA J*. **46 (9)** 2293-2305.
[12] Xu C and Li L 2015 *Appl. Mech. Mater*. **722** 235-238.
[13] Kosarev I N, Aleksandrov N L, Kindysheva S V, Starikovskaia S M and Starikovskii A Y 2008 *Combustion and Flame* **154 (3)** 569–586.
[14] Starik A M, Kozlov V E and Titova N S 2010 *Combust. Flame.* **157** 313-327.
[15] Uddi M, Jiang N, Mintusov E, Adamovich I V and Lempert W R 2009 *Proc. Combust. Inst* **32** 929-936.
[16] Pancheshnyi S, Eismann B, Hagelaar G J M and Pitchford L C, available at: http://www.ZDPlasKin.laplace. univ-tlse.fr , 2008.
[17] Lutz A E, Kee R J and Miller J A, SENKIN: A FOR- TRAN Program for Predicting Homogeneous Gas Phase Chemical Kinetics with Sensitivity Analysis , Sandia National Laboratories, Report No. SAND87-8248 (1988).
[18] Capitelli M , Ferreira C M, Gordiets B F and Osipov A I, Plasma kinetics in atmospheric gases, Springer, 2000.
[19] Flitti A, and Pancheshnyi S 2009 *The European Physical Journal Applied Physics* **45 (2)** 21001.
[20] Mao X, Rousso A, Chen Q and Ju Y 2019 *Proc. Combust. Inst.* **37** 5545-5552.
[21] Mao X, Chen Q and Guo C 2019 *Energy Conversion and Management* **200** 112018.
[22] Fontanarosa F, Mehdi G, De Giorgi M G and Ficarella A, 2020 *E3S Web Conf.* **197** 10001.
[23] Mehdi G, Bonuso S and De Giorgi M G 2021 *Energies* **14** 5814.